FORSCHUNGSZENTRUM ROSSENDORF FZR

FZR-198
November 1997
Preprint

Archiv-Ex.:

C.-M. Herbach, H.-G. Ortlepp and W. Wagner
For the FOBOS collaboration

Decay study of hot heavy nuclei below the multifragmentation threshold with the FOBOS detector at Dubna

Herausgeber:
FORSCHUNGSZENTRUM ROSSENDORF
Postfach 51 01 19
D-01314 Dresden
Telefon (03 51) 26 00
Telefax (03 51) 2 69 04 61

Als Manuskript gedruckt
Alle Rechte beim Herausgeber

Decay study of hot heavy nuclei below the multifragmentation threshold with the FOBOS detector at Dubna

C.-M. Herbach , H.-G. Ortlepp and W. Wagner
for the FOBOS * collaboration -
Joint Institute for Nucler Research, Dubna, Russia,
Research Center Rossendorf Inc., Germany
Hahn-Meitner Institut Berlin GmbH, Germany,
Laboratory for Technical Developments and Applications, Sofia, Bulgaria
Moscow Engineering Physics Institute, Moscow, Russia,
Henryk Niewodniczanski Institute of Nuclear Physics, Cracow, Poland,
Omsk State Railway Academy, Omsk, Russia.

Invited talk at the
VI International School-Seminar on Heavy Ion Physics
Dubna, Russia, September 22-27, 1997

Abstract

The first series of experiments at the FOBOS detector, using beams of the U-400M cyclotron of the Flerov Laboratory of Nuclear Reactions, was devoted to few-fragment decays of equilibrated systems. To exclude deep inelastic collisions or quasifission as sources of massive fragments, hot heavy nuclei were produced in the very asymmetric reactions ^{7} Li (43 AMeV) + ^{232} Th, ^{14} N (34 AMeV) + ^{197} Au, and ^{14} N (53 AMeV) + ^{197} Au, ^{232} Th. Two- and three-fragment events were analysed on the base of masses and velocity vectors measured independently for each fragment. The events were sorted into excitation energy bins according to the linear momentum transfer following the massive transfer approach. Binary events were treated as fission. Fragment mass distributions as well as total kinetic energies were studied for an excitation energy range of 100 - 500 MeV. A new TKE parametrisation is proposed extending the Viola systematics to large mass asymmetries. With rising excitation energy the mass dispersion develops unexpectedly. Two new effects have been found and are discussed as consquences of the cooling down during the slow fission process at moderate E*, and of a strong decrease of the fission time at large E*. Ternary events were analysed by comparing measured velocity correlations with results of Coulomb trajectory simulations. If one fragment has intermediate mass (A = 10...30), two components in the relative velocities and the Z/A ratios confirm a sequential and a neck mechanism. For events with three fragments of comperable size neither the assumption of two sequential independent fission acts nor a multifragmentaion-like scenario can reproduce the data. Agreement is achieved if these three-fragment decays are characterized by a collinear intermediate state followed by two scissions separated by no more than 200 fm/c, a very short time scale compared with usual saddle-to-scission intervals.

*The FOBOS project has been supported by the BMBF, Germany, contracts Nr. 06 DR 100, and 06 DR 671

Introduction

Nuclear reactions in the Fermi energy domain are characterized by a complicated interplay of different processes between the first touching of the two nuclei and the creation of the final products. The aim of the present study is to separate one as clear as possible stated question: How develops the decay of a hot equilibrated nucleus into a few massive fragments if the excitation energy is stepwise rised from about 100 to 500 MeV? Other mechanisms delivering fragments like deep inelastic collisions and quasifission should be avoided to not confuse the analysis. To exclude spinodal instabilities as sources of fragments a compression-expansion mechanism should be avioded too. We bombarded heavy targets (Au, Th) with light projectiles (Li, N) in the Fermi energy region. At our bombarding energies the incomplete fusion mechanism [1] leads to a broad distribution of excitation energies. A selection in bins of the linear momentum transfer (LMT), however, allows to derive mean excitation energies applying the masive transfer approach [2] and to analyse the fragment observables within these groups.

Reactions and measured quantities

The measurement was performed at the beam of the Heavy ion isochroneous cyclotron U-400M [3] in the Flerov Laboratory of Nuclear Reactions of the JINR Dubna. The reactions ^{7}Li (43 AMeV) + ^{232}Th, ^{14}N (34 AMeV) + ^{197}Au, as well as ^{14}N (53 AMeV) + ^{197}Au and ^{232}Th were studied. Thin target of 150 - 300 $\mu g / cm^2$ deposited on 30 - 60 $\mu g / cm^2$ Al_2O_3 or C backing in the center of the 4π-fragment-spectrometer FOBOS [4] were bombarded with beams of 2 - 3 $\times 10^9$ ions /s.

The fragments were recorded in combined detector modules of large opening angle placed at 50 cm from the target. Each module consisted of a position-sensitive avalanche counter and an axial field (Bragg-) ionization chamber which measured the coordinates (ϑ,φ), the time-of-flight (TOF), and the residual energy (E) of the fragments. The flight time reference was taken either from small transmission avalanche counters placed 12 cm from the target in the direction of two of the modules, or from the cyclotron RF.

From the measured quantities the individual fragment masses (M_f) and the momentum vectors (p_f) were derived applying the TOF-E method "event by event" without any kinematic assumption. For every binary or ternary event also further interesting quantities, like LMT, fragment mass sum ($\Sigma(M_f)$), folding angle, fragment momentum vector sum ($\Sigma(p_f)$), relative velocities and others are determined. The kinematics of fission after incomplete fusion is illustrated on the velocity diagram shown in Fig. 1.

In the first reaction step - incomplete fusion + pre-scission evaporation - the system just before scission has the velocity v_Σ. In this frame the fragments have the velocities C-A and C-B. If only $v_{lab\ 1}$ and $v_{lab\ 2}$ are measured (kinematic coincidence method [5]), the transversal component of v_Σ cannot be determined and the incorrect velocities C'-A and C'-B are used to derive the masses. In our analysis the mass determination is independent of v_Σ and v_Σ itself follows from $\Sigma(p_f) / \Sigma(M_f)$. This Principle allowes a more accurate analysis of fragment mass and total kinetic energy distriburtions in dependence on the excitation energy derived from the linear momentum transfer. A sufficient large value of $\Sigma(M_f)$ together with a limited deviation of the direction of the vector $\Sigma(p_f)$ from the beam direction were used as

criteria for the selection of binary decays. The same seletion criteria were applied also for ternary events with the sums taken over three fragments.

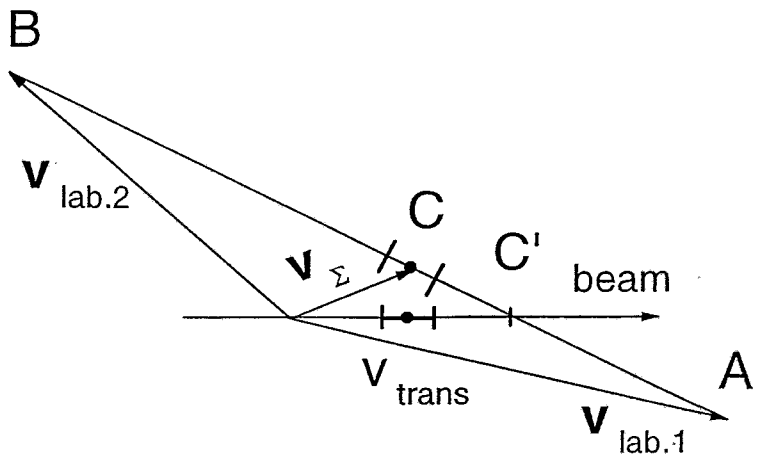

Fig. 1. Velocity diagram of the investigated reaction. The lab. velocities v_{lab1} and v_{lab2} are the result of the fission of a nucleus moving with v_{Σ} (see text).

Total kinetic energies up to very asymmetric binary decays

Evaluations of the total kinetic energy release (TKE) in fission [6, 7] are widely used for prediction and interpretation purposes of nuclear-reaction data. The TKE-formula of ref. [7], which bases on a simple two-spheres approximation of the scission configuration, well describes the measured mean TKE of mass-symmetric as well as medium-asymmetric fission, if a correction for the charge split and the actual fragment radii is applied. At large fragment mass asymmetries ($R = A_2 / A_1$) observed in the binary fragmentation of hot compound systems produced by incomplete fusion reactions (e.g. in refs. [8, 9, 10]), however, the scaling of the effective scission distance ($\sim (A_1^{1/3} + A_2^{1/3})$) becomes incorrect. The TKE smoothly approaches to the energy value of the Coulomb barrier. This means that the fission path of the nucleus from the saddle towards scission becomes successively shorter, and the collective motion is, with respect to symmetric fission, less damped [8]. Such a behaviour has been predicted in ref. [11].

Analyzing the TKE-A distributions measured at FOBOS in the reaction ^{14} N (34 AMeV) + ^{197} Au [8] we empirically found that the TKE measured for binary fragmentations can be rather accurately described over the broad range of R by the parametrization given in eq. 1.

$$TKE = c \cdot \frac{Z^2}{A_1^{1/3} + A_2^{1/3} - A^{1/3}} \cdot \frac{A_1 A_2}{A^2} \text{ MeV} \qquad c = (0.2904 \pm 0.0075) \qquad (1)$$

In the case of symmetric mass split, eq. 1 reduces to the analytic expression given in refs. [6, 7], but without the constant term and with a slightly different slope parameter. As the further analysis showed, eq. 1 also well evaluates the experimental TKE-data of refs. [9, 10] over a wide mass range of fissioning nuclei and fragment asymmetries (fig. 2).

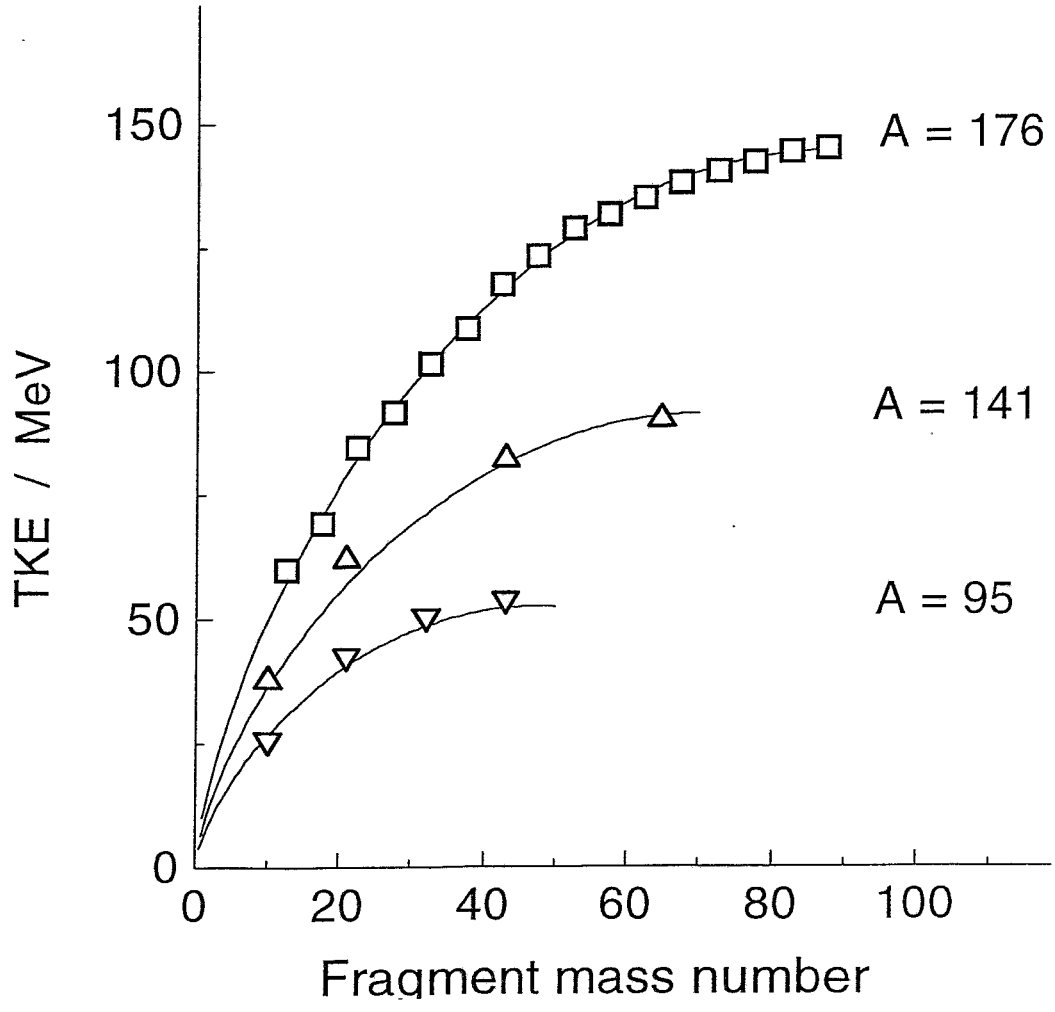

Fig. 2 Experimental TKE-data from FOBOS (ref. [8], squares) and from GSI measurements in the lower A region (refs. [9, 10] (triangles) compared with calculations using eq. 1 (lines)..

Narrow fragment mass distributions at E* ≈100 - 200 MeV - a new effect caused by a dynamical fission time-scale

In a new analysis of the data taken earlier for the reaction ^{7}Li (43 AMeV) + ^{232}Th [12, 13] distortions of mass distributions due to acceptance and error correlation effects were excluded. Mean LMT-, single FF-mass- and mass-sum spectra were created for five data-subsets.

The decrease of the FF mass-sum with increasing LMT (fig.3) is caused by the enhanced particle evaporation. The value of 13 MeV per lost a.m.u. well agrees with that from direct mea-surements of the particle multiplicities [14], indicating that the mass determination is correct.

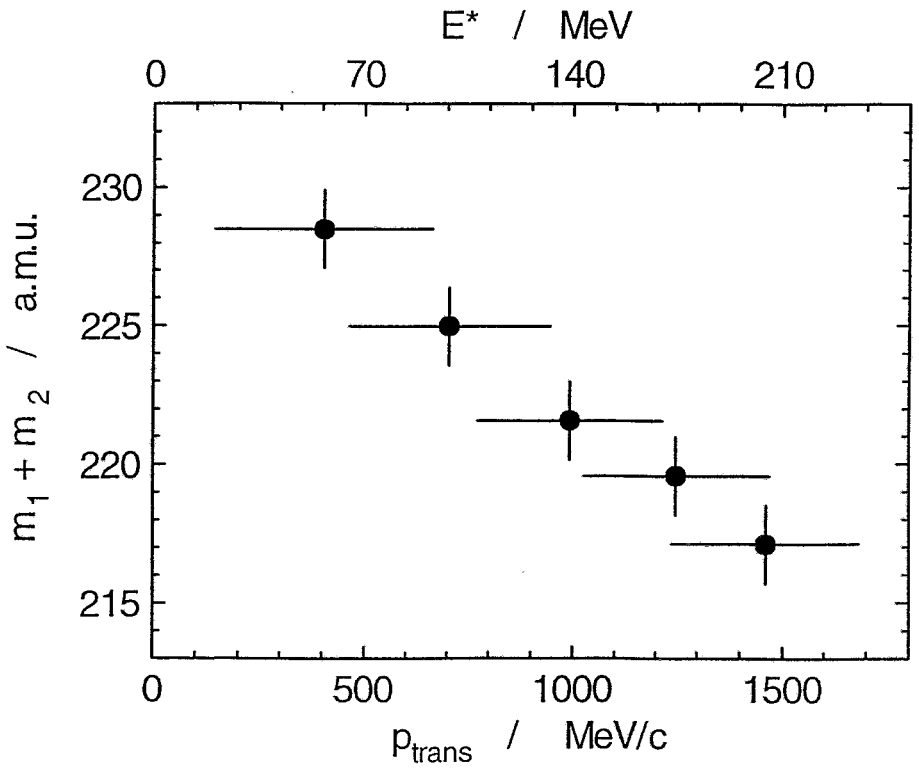

Fig. 3: Sum-mass of the fission fragments versus the linear momentum transfer.

A double-humped component was found in the single FF-mass spectra at lowest LMT. Since in the present analysis we are only interested in the symmetric liquid-drop part, a further selection was performed by cuts of the total kinetic energy (TKE) (fig. 4). In agreement with the results obtained for light Th isotopes in ref. [15], at TKE < 165 MeV the asymmetric component is suppressed

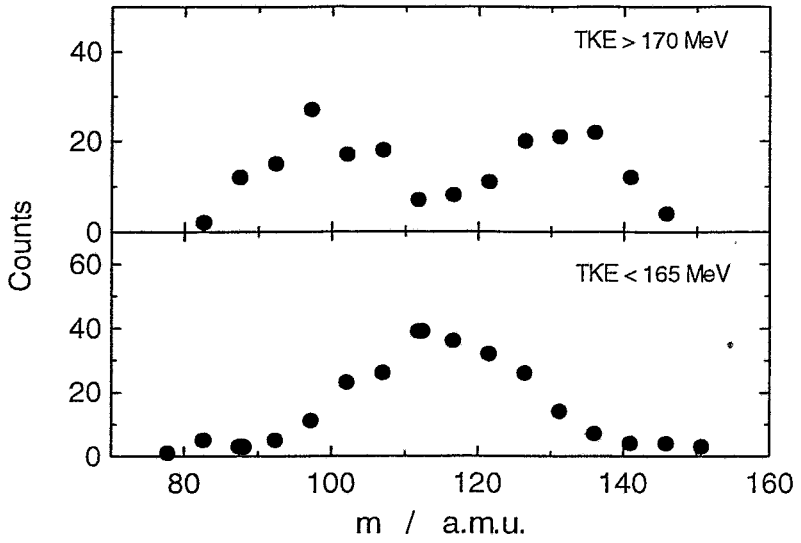

Fig. 4: Fission fragment mass spectra at lowest LMT separated by two TKE-cuts.

The fragment-mass dispersions (σ_m) deduced in this way are shown in dependence on the LMT in fig. 5.

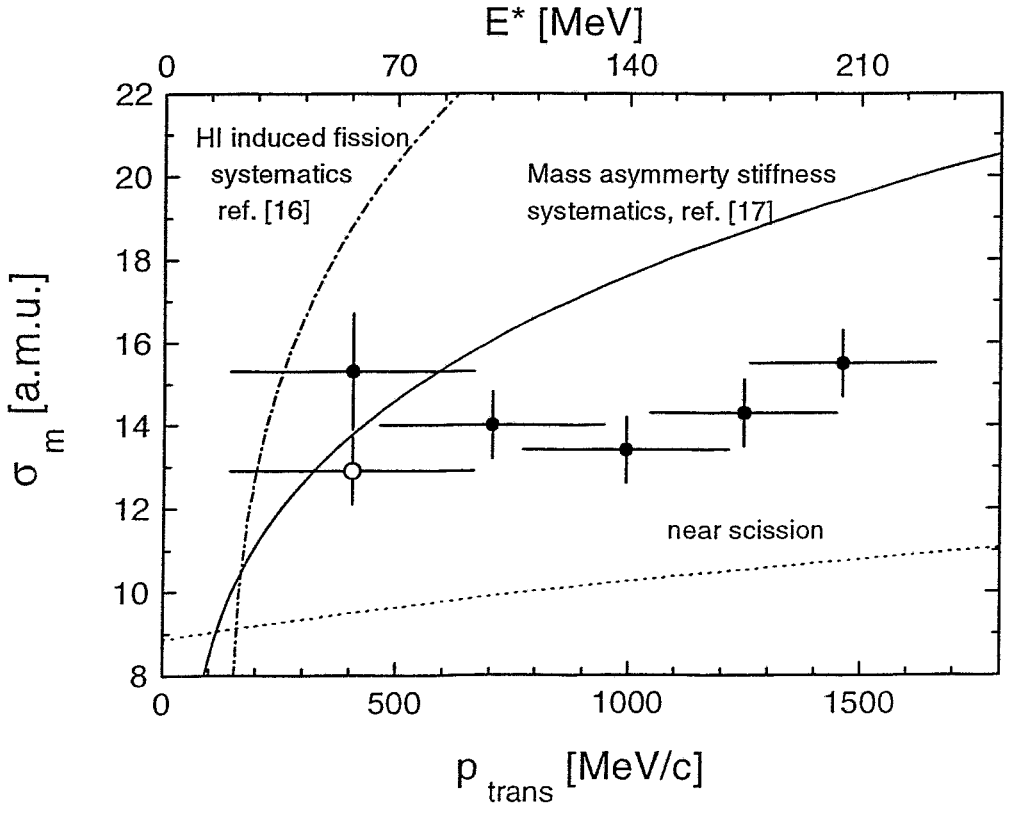

Fig. 5 FF-mass dispersion in dependence on E* derived from the LMT. The value for the symmetric component separated at lowest LMT is shown by the open circle (lines – see text).

They lie far below the systematics derived on the base of heavy-ion induced fission data in ref. [16], thus demonstrating the effect of suppression of the upper mentioned experimental errors by our analysis method.

At $E^* = 50 \div 90$ MeV the measured σ_m are well described via the nuclear temperature Θ and the mass- asymmetry stiffness parameter q [17].

$$\sigma_m^2 = \Theta / q \qquad (2)$$

Although it has already been shown in 1970, that the liquid-drop predictions of q cannot describe the measured data at $Z^2 / A > 32$ [18], eq. 1 holds if an effective q is introduced, accounting for the saddle-to-scission dynamics. The diffusion model [19] is able to predict a correct effective q. The rise of σ_m at $E^* > 90$ MeV, predicted by eq. 1 using q from the experimental systematics of ref. [17], is also shown in fig. 5.

We found that the rise of σ_m at $E^* > 80$ MeV is considerably smaller. This fact can be interpreted as an effect of the particle evaporation continuing during the descent from the saddle to scission. The *effective* Θ determining the final σ_m, therefore, becomes lower than the initial Θ.

The experimentally determined prior-to-scission neutron multiplicities are subdivided into a pre-saddle- and a descent component in ref. [20]. One can estimate that at $E^* \geq 100$ MeV the energy removed by the descent neutrons exceeds the energy gained by the effective fission Q-value. Therefore, the narrowness of the mass distribution observed up to $E^* \bullet 200$ MeV is a further confirmation of the relatively long saddle-to-scission transient time, allowing the system to substantially cool down by the evaporation of light particles.

The extreme assumption, that σ_m is governed by the effective Θ at scission (formally using the systematics of ref. [21] and the near-scission LDM q from ref. [19], is also excluded by the measurement.

Fission fragment mass distributions at E* up to 350 MeV

As it is interesting to trace the behavior of the mass distributions at higher temperature, in a further experiment hot heavy nuclei excited up to 350 MeV were produced in the reaction ^{14}N (34 AMeV) + ^{197}Au. Mass distributions corrected for geometrical acceptance effects have been created in dependence on E* (fig. 6). The width of these spectra steadily increases with increasing E*. A more detailed inspection proved that the data at the smallest as well as at the largest E* can be well fitted by single Gaussians. The distributions at the intermediate E*, however, show tails resembling a two-component configuration. Therefore, these data have been fitted by a sum of *two* Gaussians, where the dispersions of the components were taken from the distributions at the extremes of E*, respectively. Such a decomposition enabled us to fit all mass distributions simultaneously (fig. 6).

The yields of the two components are plotted versus the mean E* in fig. 7. One observes that at $E^* \approx 140$ MeV the amount of the *broad component* is $\approx 10\%$. It *steadily increases* with increasing E*, whereas the yield of the narrow component reaches its maximum near $E^* = 250$ MeV and then decreases again. It seems that another mechanism of the (binary) disintegration of the hot nucleus becomes allowed above some critical E*, and it clearly dominants at $E^* \geq 300$ MeV ($E^* / A > 2.5$ MeV/a.m.u.) (fig. 7).

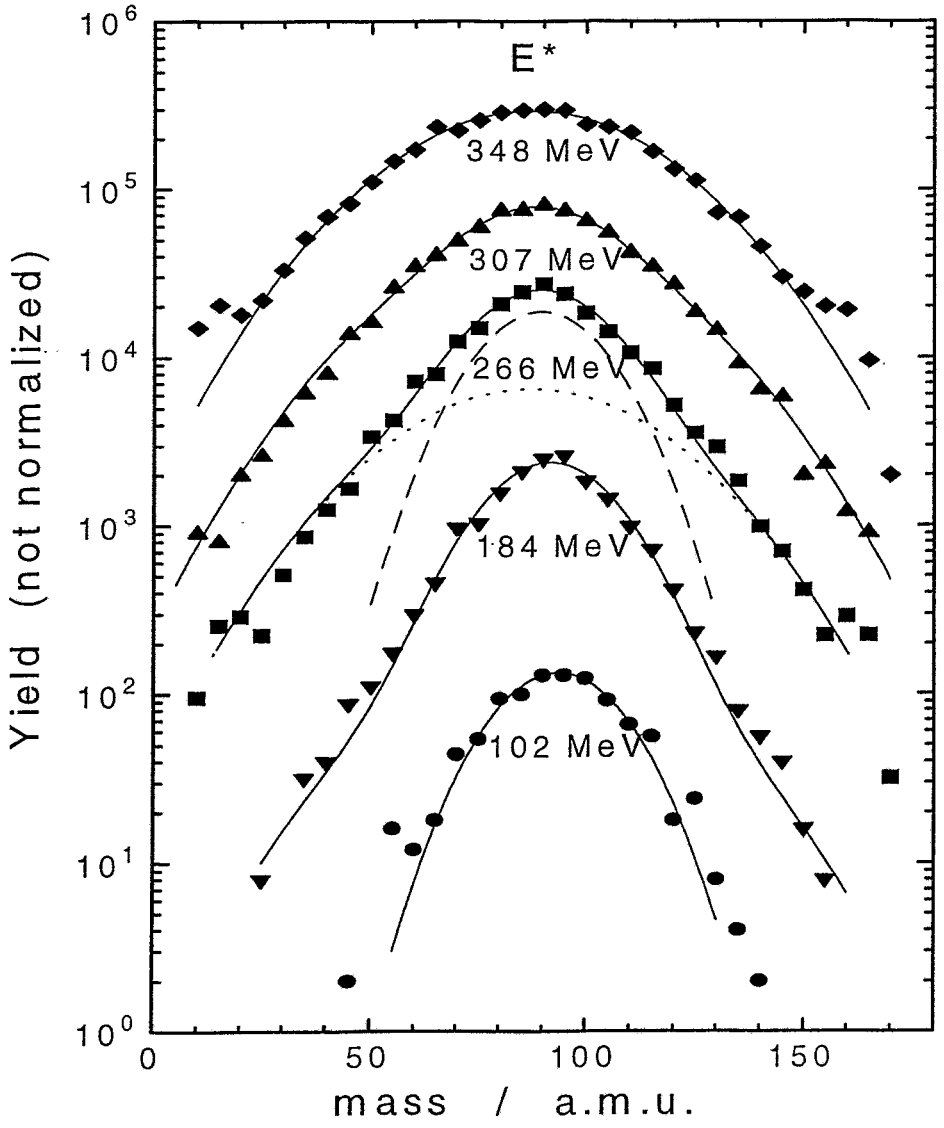

Fig. 6: Measured fragment - mass distributions (symbols) in dependence on the excitation energy (E*) for the reaction. The full lines are fits to the data (see text). The dashed and the dotted line show the narrow and the broad component, respectively, for the distribution at a mean E* of 266 MeV (squares).

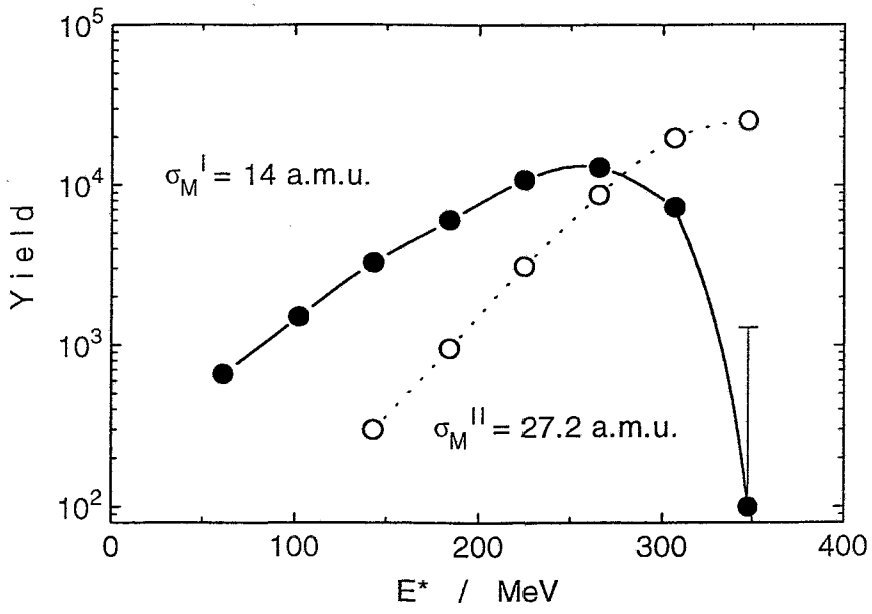

Fig. 7 Yields of the narrow (full circles) and the broad (open circles) component respectively, in dependence on the excitation energy (E*). The mass dispersions (σ_M) relate to the Gaussians fitted to the data shown in fig. 6.

Let us make an attempt to qualitatively interpret the experimental findings referring to the potential-energy surface (PES) of a fissioning system in the collective coordinates representing the elongation- and the mass-asymmetry degrees of freedom. In the framework of the statistical model (cf. ref. [11]), the probability of fission is governed by the phase-space flux over the ridge-line of conditional saddle-points. At not to high E*, the dynamics of the decay process together with the competing particle evaporation (see above) cause a channeling of this flux along the valley of symmetric fission. Assuming a static PES, the broad component could then be understood as a *"flux over the whole ridge-line"*, which should be energetically allowed at sufficiently large E*. Since there is a variety of possible fission trajectories from the ridge-line to the line of the conditional scission-points, the mass dispersion of the broad component should be strongly influenced by the entire shape of the potential-energy surface.

The only difference between the two components observed then would really consist in the partition of the mass-asymmetric splitting — *but why* the particle evaporation succeeds to cool down the system before it fissions at low E* (100...200 MeV, see above), but does not at high E* (> 250 MeV) where the evaporation width (Γ_n) is substantially larger ? Is this a hint, that the process responsible for the broad component proceeds faster than that producing the narrow component ? (cf. ref. [22]). Even if one assumes that there is not any cooling , the large value of σ_M^{II} observed (fig. 6, 7) can not be obtained neither by the approach of ref. [11] nor by that of refs. [17, 19]. This, however, means that the PES must change with increasing E*. Such a hypothesis has already been discussed in ref. [23] quoting equation-of-states arguments. If at higher E* the surface tension of a hot nucleus would reduce, the *effective* fissility would increase, and the mass-asymmetry stiffness would decrease (cf. refs.

[17, 19]) allowing in this way a more asymmetric mass splitting. The transfer of more angular momentum in more violent collisions also leads to a higher effective fissility. The vanishing of any stability against mass-asymmetric divisions at very high E* (cf. ref. [24]) resembles the approaching to the Businaro-Gallone point at low fissility.

Two modes of IMF - accompanied fission

The three-body decay of hot heavy nuclei with excitation energies of up to 3.5 AMeV was investigated using the reactions ^{14}N (53 AMeV) + ^{197}Au and ^{232}Th. Intermediate mass fragments (IMF; Z > 2) have been recorded in coincidence with fission fragments (FF). The separation of IMF was carried out with the help of windows set in the two-dimensional distribution of the yield over the relative velocity between the IMF and the center-of-mass of the two FF (v_{IMF-FF}), and the IMF-emission angle relative to the fission axis (Θ_{IMF-FF}) (fig. 8).

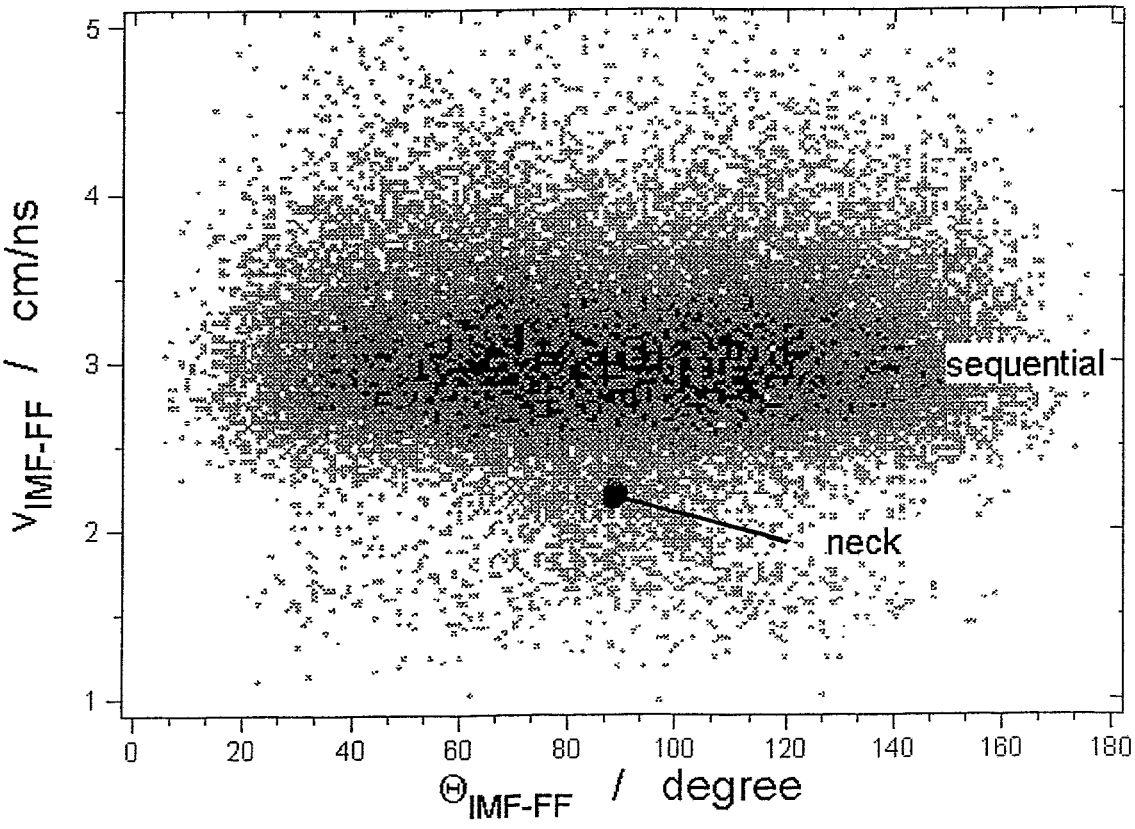

Fig. 8: Relative IMF-velocities versus the emission angle of the IMF relative to the fission axis.

The dominant isotropic yield corresponds to the Coulomb repulsion from a target-like nucleus with $v_{IMF\text{-}FF} = 2.5 \div 3.5$ cm/ns. In contrast to that, IMF emitted in the range of $v_{IMF\text{-}FF} = 1.5 \div 2.3$ cm/ns are focused close to $\Theta_{IMF\text{-}FF} = 90°$, thus confirming the neck-emission mechanism of IMF recently observed for $Z \leq 8$ in refs. [25, 26]. A fragment generated between the two other FF can be identified by its reduced kinetic energy and the Coulomb focusing perpendicular to the fission axis.

Three further observations in our data confirm the neck emission mechanism of the low velocity IMF component:

(i) The rise of the yield with increasing E* is less steep because only a small part of the initial E* remains at the late stage when they are created.

(ii) Its mass distribution is considerably broader than that of the other component and contradicts with the assumption of statistical emission from a target-like nucleus.

(iii) The neck IMF have a larger N/Z - ratio (fig. 9). The maximum yield of IMF sequentially emitted by the hot nucleus is in accordance with the line of β-stability, the N/Z - ratio of neck-particles is nearly that of the compound nucleus.

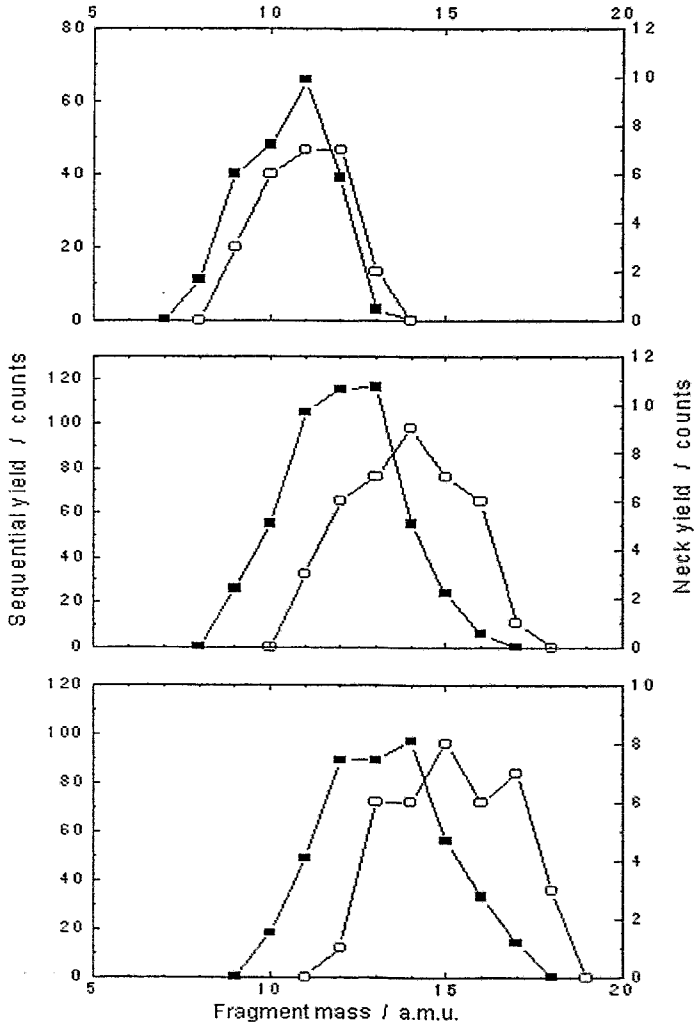

Fig. 9:

Mass distributions of IMF (Z = 5, 6, 7 from top to bottom) emitted sequentially (squares : left scale) and from the neck region(circles: right scale).

(The isotopic distributions are broadened due to the experimental mass resolution.)

Mass-symmetric tripartitions

Selected events of nearly mass- symmetric tripartitions presently are further analyzed and compared with Coulomb trajectory calculations. The assumption of two independent fission acts separated by a certain time difference τ_{12} does not reproduce the measured angular and velocity correlation for any assumed value of τ_{12}. A Coulomb energy reduced by 15% must be assumed for the first fission. This means that the first scission configuration is more deformed than in binary fission. From this and also from the small value of τ_{12} = 100 - 200 fm/c needed for best agreement we conclude that the second fission is already in progress at the first scission instant. Only an large elongation of the second fissionig system approximately in the direction of the first first scission axis can explain the observed 15% reduction of the Coulomb energy. Therefore, there must exist an intermediate state with a similar chain shape like considered long ago in ref. [27], but up to now not confirmed experimentally for heavy-ion induced fission. For the second scission best agreement is achieved assuming the exact Viola [6] Coulomb energy. From this finding we conclude that the second separation is usual fission and, therefore, the whole process cannot be a multifragmentation out of an expanded state. Furthermore, above a threshold of about 200 MeV our experimental yield of such decays remains nearly constant in contradiction with an expected steep rise if one assumes statistical multifragmentation.

References

[1] V.E. Viola, Jr. et al., Phys. Rev. C26 (1982) 178

[2] D. Guerreau, Int. School on Nucl. Phys. „Nuclear Matter and Heavy Ion Collisions", Les Houches, France, 1989, Report GANIL P 89-07, Caen, 1989

[3] G.G. Gulbekian and V. B. Kutner, Proc of the FOBOS Workshop '94, Cracow, Poland, 1994, FZR-65, Rossendorf 1995, p. 25.

[4] H.-G. Ortlepp et al., FZR-181, Rossendorf 1997 (to be published in Nucl. Instr and Meth.)

[5] G. Casini et al., Nucl. Inst. and Meth. A277 (1989) 445.

[6] V.E. Viola, Jr., Nucl. Data Tab. A1 (1966) 391.

[7] V.E. Viola et al., Phys. Rev. C31 (1985) 1550.

[8] W. Wagner et al., in: "Advances in Nucl. Dynamics 2" (eds. W. Bauer and G.D. Westfall) Plenum Press, New York, 1996, p. 341.

[9] R.J. Charity et al., Nucl. Phys. A483 (1988) 371.

[10] R.J. Charity et al., Nucl. Phys. A511 (1990) 59.

[11] L.G. Moretto et al., in: "Progr. in Part. and Nucl. Physics", vol. 21 (ed. A. Faessler) Pergamon Press, Oxford, 1988, p. 401.

[12] H.-G. Ortlepp et al., Proc. Int. Conf. LEND '95, St. Peterburg, 1995
(Eds. Yu. Oganessian, R. Kalpakchieva, W. von Oertzen)
World Scientific, Singapore, 1995, p. 231.

[13] C.-M. Herbach, Proc. FOBOS workshop'94, Cracow, Poland, 1994 (Ed. W. Wagner)
FZR-65, Rossendorf, Germany,1995, p. 87.

[14] E.C. Pollacco et al., Phys. Lett. B146 (1984) 29.

[15] G. Chubarian et al., Phys. At. Nucl., v. 56 (1993) 3.

[16] W.U. Schröder and J.R. Huizenga, Nucl. Phys. A502 (1989) 473c.

[17] M.G. Itkis et al., Phys. Elem. Part. At. Nucl., v. 19, (1988) 701.

[18] S.A. Karamyan et al., Phys. At. Nucl., v. 11 (1970) 982.

[19] G.D. Adeev et al., Phys. Elem. Part. At. Nucl., v.19 (1988) 1229

[20] I.I. Gontchar, Phys. Elem. Part. At. Nucl., v. 26 (1995) 932.

[21] D. Hilscher and H. Rossner, Ann. Phys. Fr. 22 (1992) 471.

[22] W. Wagner et al., Proc. 3^{d} Int. Conf. on Dynamical Aspects of Nucl. Fission, Casta-Papiernicka, Slovak Rep., 1996 (Ed. J. Kliman, B.I. Pustylnik); Dubna 1996, p. 104, FZR-163, Rossendorf, Germany,1997.

[23] V.A. Karnaukhov, JINR E7-96-182, Dubna, 1996.

[24] G. Klotz-Engmann et al., Nucl. Phys. A499 (1989) 392.

[25] Fields D.E. et al., Phys. Rev. Lett., v. 69, 1992, p. 3713.

[26] Chen S.L. et al., Phys. Rev., v. C54, 1996, p. 2114.

[27] Diel H. and Greiner W., Phys. Lett., v. B45, 1973, p. 35.